Experimental validation of Reference Chip Antennas for 5G Measurement Facilities at mm-Wave

A. Giacomini, L. Scialacqua, F. Saccardi, L. J. Foged
Microwave Vision Italy s.r.l.
Via dei Castelli Romani, 59
00071 Pomezia, Italy
andrea.giacomini@mvg-world.com

E. Szpindor, W. Zhang, M. Oliveira, P. O. Iversen
Orbit/FR Inc.
650 Louis Dr., Suite 100
Warminster, 18974, PA, USA
peri@orbitfr.com

J. M. Baracco
MARDEL
2423 Av. Emile Hugues
06140 Vence, France
jmb.mardel@wanadoo.fr

***Abstract*—In this paper, the experimental validation of a micro-probe fed reference antenna targeting the upcoming 5G applications (24.25-29.5GHz band) is presented. The main purpose of these reference antennas is to serve as "gold standards" and to perform gain calibration of 5G test facilities through the substitution method. The outline of these antennas is based on a square array of four printed patches enclosed in a circular cavity. The RF input interface is a stripline-to-coplanar waveguide transition and allows for feeding the device with a micro-probe. Performance obtained by high-fidelity modeling is reported in the paper and correlated to experimental data. Interaction and unwanted coupling with the test equipment are discussed. The use of echo-reduction techniques and spatial filtering is investigated to mitigate these effects.**

I. INTRODUCTION

The expanding market for 5G applications at mm-wave is pushing the measurement industry to develop new test equipment. For such applications, small active array antennas are becoming more and more popular within the industry, based on technology and signal processing concepts previously developed for 4G and MIMO applications. These antennas are usually compact in size and do not have connectorized RF interfaces. The feeding is in general carried out by means of micro-probes. Dedicated test equipment with suitable probing stations is required to characterize these devices. In order to calibrate these facilities in gain using the substitution method and assess measurement accuracy, standard reference antennas with reliable performance are needed.

In this paper, the experimental validation of a micro-probe fed reference antenna targeting the upcoming 5G applications (24.25-29.5GHz band) is presented [1]. Details of the operating bands in up/down-link and frequency allocation is recalled in Table I. The outline of this reference antenna is based on a square array of four printed patches enclosed in a circular cavity. The patches are fed by capacitive coupling by an integrated strip-line beam forming network. The RF input interface is a stripline-to-coplanar waveguide transition and allows for feeding the device with a Ground-Signal-Ground (GSG) micro-probe.

Performance obtained by high-fidelity modeling is reported in the paper and correlated to experimental data by pattern comparison and performance indicators. Manufacturing repeatability is also quantified using statistical means over a medium quantity batch of antennas. Interaction and unwanted coupling with the test equipment are also addressed. The use of echo-reduction techniques is also investigated to mitigate these unwanted effects.

The paper is organized as follows: Section II contains a description of the hardware characteristics of the chip reference antennas; Section III summarizes the measurements results; Section IV reports on data-processing; finally, comments and conclusions are given in Section V.

TABLE I. NEW RADIO OPERATING BANDS.

Operating Band	Uplink (UL) *Base Station RX* *User Equipment TX*	Downlink (DL) *Base Station TX* *User Equipment RX*
n257	26.5 – 29.5GHz	26.5 – 29.5GHz
n258	24.25 – 27.5GHz	24.25 – 27.5GHz
n261	27.5 – 28.35GHz	27.5 – 28.35GHz

II. HARDWARE DESCRIPTION

The reference chip antenna is a 2x2 square array of cavity backed patch antennas surrounded by a choke ring, fed by a strip-line corporate beam-forming network (BFN). Details of the RF design can be found in [2]. The reference chip antenna "as-built" is shown in Figure 1. , in its two configurations: Zenith and Nadir looking, depending on the main direction of radiation pattern with respect to the input RF feeding point. The overall dimensions are *1.5'' x 1.5''*, with an octagon shaped envelope to allow for accurate alignment in the measurement set-up. A metal cladding has been bonded to the ground-plane of the printed circuit board (PCB), to provide flatness and robustness, reaching

an overall thickness *0.11''*. The radiating surface is gold plated with enough thickness to ensure durability for a consistent number of probe landings (at least 1000). Antennas are individually marked to guarantee traceability of the standard, without affecting performance.

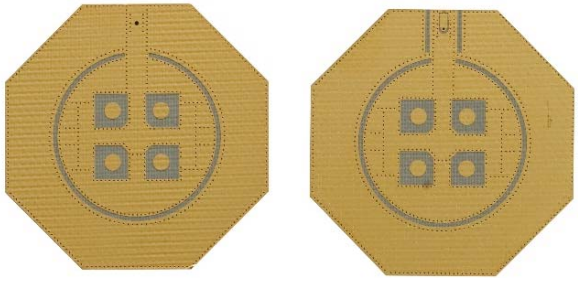

Figure 1. Reference Chip Antennas in Nadir (left) and Zenith (right) configuration.

The construction is based on a stack of two layers, bonded by a thin adhesive ply. The top layer is a single-sided PCB accommodating the radiating elements and the top ground plane. The bottom layer is a thinner double-sided PCB with the corporate strip-line BFN on one side and the bottom ground plane on the other. High quality laminate materials [3] have been selected for manufacturing, with an appropriate adhesive ply of matched dielectric constant.

The input RF interface of the device is a coplanar waveguide (CPW) etched on the top ground plane (for the Zenith looking version), designed to allow the landing of a *200* µm pitch Ground-Signal-Ground (GSG) probe, but also accepts a larger probe tip. Details of the nominal micro-probe tip are shown in Figure 2.

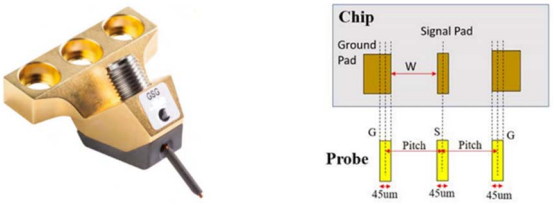

Figure 2. Example of a GSG micro-probe and details of the landing pad requirements.

The CPW input stepped transition for the Zenith looking configuration is depicted in Figure 3. (microscope view) with the GSG micro-probe tip perfectly landed on the chip pads.

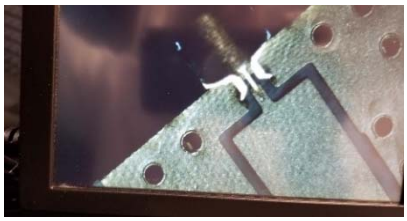

Figure 3. Microscope view of the landed micro-probe tip.

III. Measurement Results

A medium quantity batch (approx. 10 units) of these chip reference antennas have been constructed and underwent verification testing to qualify the design, asses the repeatability of the manufacturing process and derive reliable performance data. The main purpose of these antennas is to serve as gain calibration standards for spherical near/far-field measurement systems in the *24.25-29.5*GHz band. The widely used gain transfer method (substitution method), requires the use of a reference antenna with known and reliable gain characteristics. The AUTs have been referenced in the measurement campaign with their own part numbers: SGCA-27-U-H (Zenith) and SGCA-27-L-H (Nadir).

The measurement campaign for conducted and radiated performance has been carried out in the µ-Lab shown in Figure 4. In this set-up, the probe antenna rotates in θ and ϕ over the sphere surrounding a stationary micro-probe assembly [3]. A low-density foam "chuck" supports the Antenna Under Test (AUT) during the test and the AUT is fed by the micro-probe station through a coplanar waveguide (CPW). The measurements have been carried out in the nominal band (*24.25-29.5*GHz) and slightly extended in frequency to verify out-of-band performance.

Figure 4. µ-Lab: mm-wave Spherical Near-Field measurment facility.

A. Conducted measurements

After metrological alignment and planarization of the contact pads of the GSG micro-probe (model ACP65-A-GSG-200) [5], the test set-up has been calibrated for reflection coefficient measurement using an Impedance Standard Substrate (ISS Cal Kit model 143-033) [6]. The measurement of the input reflection of the AUTs served as pass/fail acceptance testing, in order to reject devices with major manufacturing defects. As a result, it was found that most of the tested antennas (approx. 90%) was accepted. An example of AUT being measured for input reflection coefficient is shown in Figure 5.

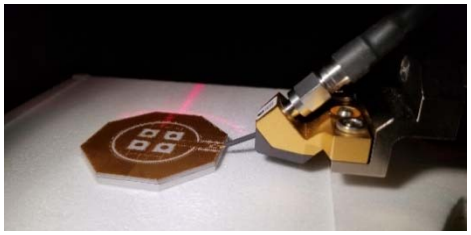

Figure 5. SGCA-27-U-H reference antenna under test.

The measured results referenced to 50Ohms are presented in Figure 6. for SGCA-27-U-H and Figure 7. for SGCA-27-L-H. The measured traces are compared with simulated performance resulting from high-fidelity modeling [2]. The comparison is in general favorable, with an average level of input reflection in-line with expectations. It should be noted, that the modeling does not account for the presence of the micro-probe station and is excited by an ideal waveguide port. For SGCA-27-U-H, a modest frequency shift of approx. 2% is experienced. This kind of effect is fairly common in PCB design and is likely to be caused by some uncertainty in the knowledge of the dielectric constant [3], by datasheet +/-0.1 on nominal value of 3.5.

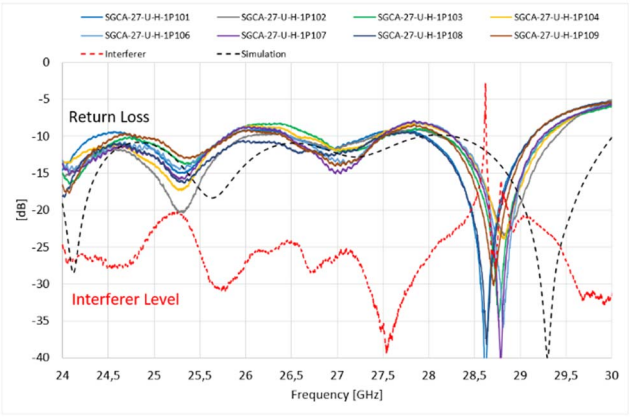

Figure 6. SGCA-27-U-H: measured return loss (wrt 50Ohms) for a batch of eight units.

For the SGCA-27-L-H, the agreement with simulated values is slightly more affected by the presence of the dielectric chuck. This support has low dielectric constant (approx. 1.1) [7] but is in physical contact with the radiating surface of the antenna.

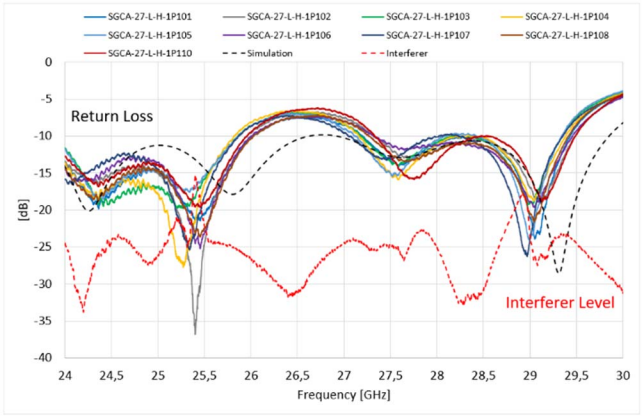

Figure 7. SGCA-27-L-H: measured return loss (wrt 50Ohms) for a batch of nine units.

For the acquired traces, the interference level associated to manufacturing and test uncertainties has been calculated [8]-[9], referenced to the average measured curve of the batch. These levels are used as performance indicators of the reliability of the constructive process. They have been found in-line with background experience for these antenna types based on kind of antennas based on PCB technology, except in the frequency range where deep resonances are measured. In these intervals, the interferer level becomes insignificant.

B. Radiated measurments

Two reference antennas have been selected for testing the radiation pattern characteristics, one in Zenith configuration (SGCA-27-U-H-1P101) and one Nadir (SGCA-27-L-H-1P102). Figure 8. shows the AUT is the measurement facility (left) and the details of the alignment means (right), that allows to place easily the device in the center of the measurement sphere. As previously mentioned, the probe antenna rotates in θ and ϕ over the sphere surrounding a stationary micro-probe assembly.

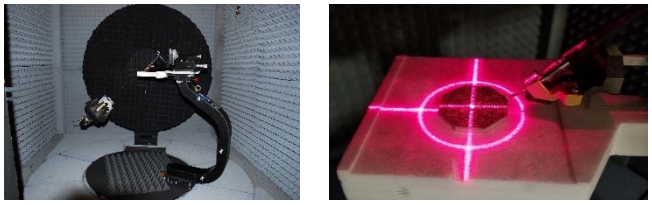

Figure 8. SGCA-27 reference antenna under test in the µ-Lab (left) and alignment means (right).

The test distance in the considered set-up is approx. 30cm, which, for the frequency band and the size of the devices does not satisfy the Far Field criteria [9]. The Spherical Near Field (SNF) dataset has therefore been expanded to Far Field by NF/FF transformation [10]. Modal filtering was applied considering a minimum sphere of 2.1cm in radius (equivalent to the physical envelope of the AUT), in order to mitigate stray signals from the measurement environment.

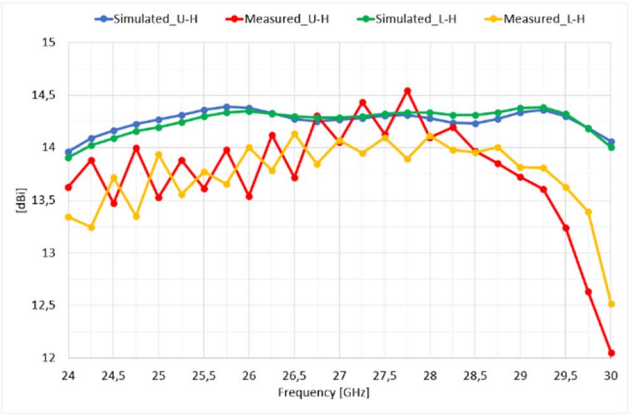

Figure 9. Boresight directivity over frequency of the SGCA-27 reference antennas: measured VS simulated.

The boresight directivity levels for both Zenith and Nadir configurations of the reference antennas are shown in Figure 9. Besides a minor frequency shift discussed in the previous section, the agreement is in general satisfactory, except for a fast-varying ripple in frequency. This oscillation is a sign of interaction between the measurement probe and the AUT. It should be noted, that the µ-Lab was conceived to test electrically

small chip antennas above 50GHz. At these test frequencies, Over-the-Air path loss is significant, and a high gain probe is required to ensure enough dynamic range. At lower frequencies (24GHz) and considering devices with large metallic ground planes (such as SGCA-27), the use of a high gain probe has the drawback of increasing the mutual coupling with the AUT, due to its large electrical size and Radar Cross Section (RCS) [11].

Measured Far Field radiation patterns normalized to directivity have been compared to simulated performance at the nominal center frequency of 27GHz. Figure 10. shows the comparison for the SGCA-27-U-H reference antenna. The shadowing effect caused by the micro-probe equipment and the positioner is clearly visible in the H-plane of the measured pattern cuts.

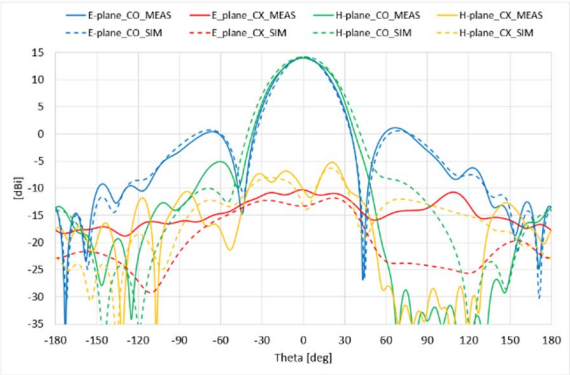

Figure 10. Directivity pattern cuts of SGCA-27-U-H: measured VS simulated @ 27GHz.

Figure 11. shows the comparison for the SGCA-27-L-H reference antenna. For this Nadir looking configuration, the radiation pattern has been re-aligned to have the main beam pointing at $\theta=0°$.

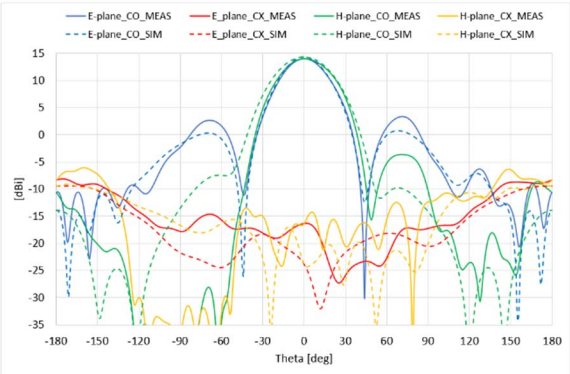

Figure 11. Directivity pattern cuts of SGCA-27-L-H: measured VS simulated @ 27GHz.

For the gain calibration of the reference antenna, the insertion loss measurement has been selected [9]. The measurement system has been calibrated through a full two-calibration at the micro-probe tip and measurement probe RF interfaces, using dedicated Open-Short-Load calibration kits. The Through calibration has been performed using a set of cables, attenuators and adapters, fully characterized. This complex procedure is strictly necessary in this case since the reference antennas are calibrated for the first time.

Realized gain over frequency is reported in Figure 12. for the Zenith looking configuration. As expected, measured gain is slightly lower than simulated and the frequency shift is still visible. It should be noted that the measured gain curve does not show ripple over frequency due to larger frequency step.

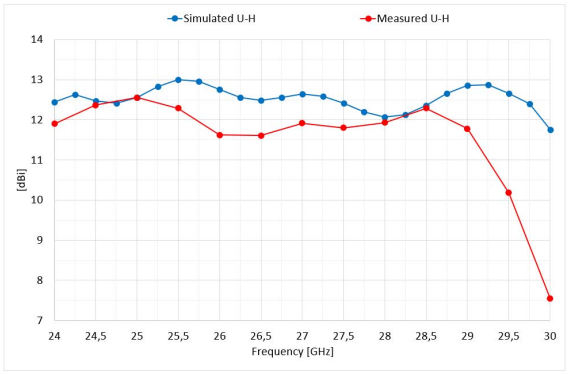

Figure 12. Realized gain over frequency of SGCA-27-U-H: measured VS simulated.

IV. Data Processing

In addition to the low-pass filtering applied to the spherical wave coefficients equivalent to a sphere enclosing the AUT only, further data processing has been considered in order to mitigate the AUT – measurement probe mutual interaction. As previously pointed out, the resulting standing wave is mainly determined by the large RCS of the measurement probe.

Two post-processing options have been evaluated: time gating and complex averaging of different datasets. The former is recommended for wideband AUTs, while the latter is more suited for narrowband devices. In the specific case of the SGCA-27, averaging two measurements acquired with different test distance (quarter wavelength @ center frequency) has demonstrated to be effective. The beneficial effects of this processing are reported in Figure 13. Peaks and valleys for the different measurement radii are inverted and the complex averaging has the effect of smoothing out the directivity curve over frequency.

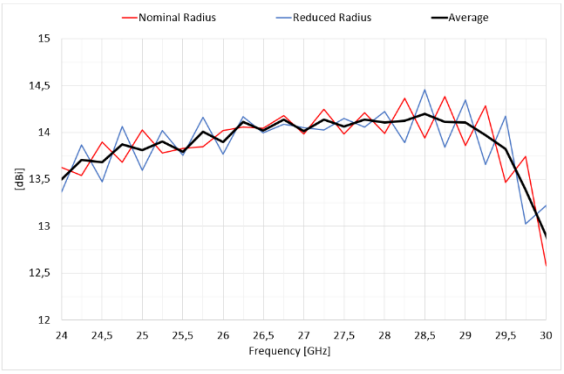

Figure 13. Boresight directivity of SGCA-27 reference antenna with averaging over the test distance.

For the Zenith configuration reference antenna (SGCA-27-U-H), spatial filtering based on Equivalent Currents [12]-[13] has been considered in order to reduce stray signals originated from the micro-probe station, such as reflected waves or direct radiation from the micro-probe tip. Reconstructed currents @ 27GHz are shown in Figure 14. (left) with a dynamic range of 40dB. Selective spatial filtering has been applied to the reconstructed box by switching off the area corresponding to the micro-probe station, as depicted in Figure 14. (right) with the grey volume.

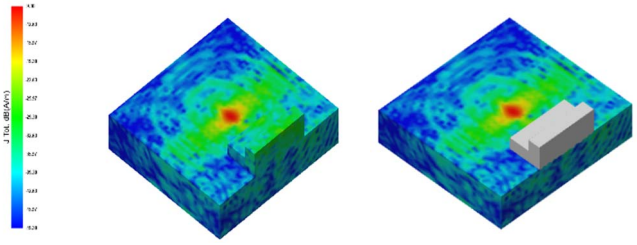

Figure 14. Electrical currents (J) reconstructed on a box enclosing the AUT and a portion of the micro-probe (left) and spatial filetring of the micro-probe (right).

Far-field patterns have been then computed w/ and w/o filtering and are presented in Figure 15. The overlay demonstrates that filtering the micro-probe does not modify significantly the radiation patterns. Also, boresight directivity over frequency has been computed with dense frequency sampling and no beneficial effect was found on the fast-varying ripple that affects the directivity over frequency curve (see Figure 9.). This was considered as a further demonstration that the AUT - measurement probe coupling is the root cause of the standing wave.

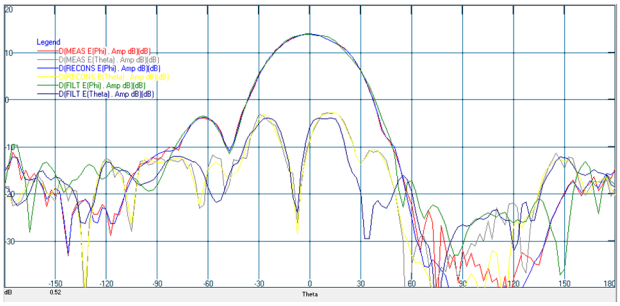

Figure 15. Directivity pattern cuts (H-plane) @ 27GHz of SGCA-27-U-H: measured (MEAS), reconstructed (RECONS) and filtered (FILT) traces.

V. CONCLUSIONS

Reference chip antennas operating at 5G mm-wave frequencies have been presented in this paper. The main purpose of these reference antennas is to perform gain calibration of 5G test facilities through the substitution method. Experimental validation of a medium quantity batch has been carried out for conducted and radiated characteristics. Correlation between simulated and measured data has been demonstrated and repeatability of the manufacturing process verified. The experimental campaign has shown the criticality of testing AUTs with large metallic surfaces (i.e. highly scattering) at short distances. In order to preserve the measurement accuracy, the need of a dedicated measurement probe with low scattering characteristics and dual polarization capabilities was confirmed by experiment.

REFERENCES

[1] 3GPP TR38.101-2 v15.2.0, "NR User Equipment (UE) radio transmission and reception - Part2: Range 2 Standalone (Rel 15)", June 2018.

[2] A. Giacomini, F. Scattone, L.J. Foged, E. Szpindor, W. Zhang, P. O. Iversen, J. M. Baracco, "Reference Chip Antenna for 5G Measurement Facilities at mm-Wave", *40th Annual Meeting and Symposium of the Antenna Measurement Techniques Association.,* 2018.

[3] https://agc-nelco.com/wp-content/uploads/2017/06/n9000a-a4.pdf

[4] E. Lee, R. Soerens, E. Szpindor, and P. Iversen, "Challenges of 60 GHz onchip antenna measurements", *IEEE International Symposium Antennas and Propagation & USNC/URSI National Radio Science Meeting*, 2015.

[5] https://www.formfactor.com/download/probe-selection-guide/?wpdmdl=2561&refresh=5d3c28e7459ab1564223719

[6] https://www.formfactor.com/download/iss-map-143-033/?wpdmdl=3180

[7] https://www.rohacell.com/product/rohacell/en/products-services/rohacell-hf/

[8] L. J. Foged, A. Giacomini, R. Morbidini, F. Saccardi, V. Schirosi, M. Boumans, B. Gerg, D, Melachrinos, "Investigation of Additive Manufacturing for Broadband Choked Horns at X/Ku Band", IEEE Antennas and Wireless Propagation Letters (Volume: 17 , Issue: 11 , Nov. 2018).

[9] Antenna Standards Committee & Near-Field Antenna Measurements Working Group, "IEEE Recommended Practice for Near-Field Antenna Measurement", IEEE Sdt 1720-2012, 2012.

[10] http://www.mvg-world.com/en/system/files/SOFT_MV-Echo_2014_bd.pdf

[11] https://www.smithsinterconnect.com/getmedia/f0b7edd1-1ef2-401a-abd5-150a2e8408a5/Scalar-and-Conical-Horn-Antennas-Series-SFH

[12] https://www.mvg-world.com/en/system/files/insight_04_19_bd2.pdf

[13] L.J. Foged, L. Scialacqua, P. Iversen, E. Szpindor, "Detection and Suppression of Scattered Fields from Coplanar Micro-Probe and Positioner in Millimeter Wave On-Chip Antenna Measurements", International Symposium Antennas and Propagation (ISAP), 2016.